Physicochem. Probl. Miner. Process., 56(2), 2020, 338-349

http://www.journalssystem.com/ppmp

Physicochemical Problems of Mineral Processing

ISSN 1643-1049

Received December 24, 2019; reviewed; accepted February 03, 2020

Adsorption of methylamine cations on kaolinite basal surfaces: A DFT study

Jun Chen [1,2,3], Fan-fei Min [1,2], Ling-yun Liu [1,2], Fei-fei Jia [4]

[1] State Key Laboratory of Mining Response and Disaster Prevention and Control in Deep Coal Mines (Anhui University of Science and Technology), Huainan 232001, China

[2] Department of Materials Science and Engineering, Anhui University of Science and Technology, Huainan 232001, China

[3] Key Laboratory of Coal Processing and Efficient Utilization, Ministry of Education, Xuzhou 221116, China

[4] School of Resources and Environmental Engineering, Wuhan University of Technology, 122 Luoshi Road, Wuhan, Hubei, 430070, China

Corresponding authors: jchen412@126.com (Jun Chen), ffmin@aust.edu.cn (Fan-fei Min)

Abstract: To explore the interaction of alkylamine surfactants with kaolinite, the density functional theory (DFT) method was used to calculate the single adsorption of different methylamine cation on kaolinite basal surfaces and the competitive adsorption of methylamine cation and water molecule on kaolinite basal surfaces, respectively. Different methylamine cations can adsorb on kaolinite basal surfaces by electrostatic interaction and hydrogen bonds, and the methylamine cations more easily adsorbed on kaolinite Si-O surface. In the case of competitive adsorption with water molecule, the methylamine cation is capable of flushing out the surrounding water molecule to get rid of its steric effect and stably adsorbing on kaolinite basal surfaces, and the adsorption state of the competitive adsorption system is more stable. The adsorption mechanism of methylamine cation on kaolinite basal surface should be the result of electrostatic interaction and hydrogen bonds, and the electrostatic interaction plays the main role.

Keywords: kaolinite, methylamine cations, density functional theory, competitive adsorption, adsorption mechanism

1. Introduction

Clays are highly muddied associated minerals (gangue) (Zhao et al., 2018; Zhang et al., 2019; Zhao et al., 2019a), and it usually exists in microparticles at less than 2 μm (Bergaya et al., 2013; Xiong et al., 2017) in most industrial mine tailings (Pendharker et al., 2017; Liu et al., 2018; Zhao et al., 2019b), which has a very adverse effect on the sedimentation (Chen et al., 2016; Chen et al., 2017), separation (Yu et al., 2017; Xing et al., 2017; Jeldres et al., 2019) and dewatering (Liu et al., 2018) of mine tailings. This is because clay mineral characterized as strong hydrophilic surfaces, extraordinarily fine granularity and strong electronegativity of the particle surfaces.

The hydrophobic modification of particle surfaces using hydrophobic surfactants is one of the main ways to generate efficient agglomeration settlement (Chen et al., 2017; Min et al., 2014) and separation (Lee et al., 2011; Huang et al., 2019) of the clay mineral particles, and improving the hydrophobicity of particle surface can further promote dewatering of the particles (Min et al., 2020). Chen et al. (2017) pointed out the adsorption of amine/ammonium salts on kaolinite surface can induce a strong hydrophobic aggregation of kaolinite particles to promote its settlement. Huang et al. (2019) used dodecyl dimethyl ammonium bromide to hydrophobic-modify the montmorillonite surface, which can effectively enhance the selective separation of montmorillonite. Min et al. (2020) pointed out hydrophobic modification can promote the high efficiency dewatering of clay particles by

DOI: 10.37190/ppmp/117769

weakening the hydration layer. Recently, the hydrophobic surfactants of alkyl amine salts (Hu et al., 2013; Jiang et al., 2014) have been studied and proven to be effective reagents for the hydrophobic modification of clay particles.

Much research has been done recently about the hydrophobic agglomeration behavior of clay particles with amine surfactants (Rodrigues et al., 2013; Shen et al., 2017; Gibsona et al., 2017), but few have actually examined the micro interaction mechanism between amine surfactants and clay particles. Therefore, it is important to analyze the microscopic mechanism of alkyl amine surfactants adsorption on clay particle surface (Peng et al., 2018). Generally, the computer simulations have employed to investigate and evaluate the adsorption mechanism of surfactants on solid surfaces recently (Rath et al., 2014; Wang et al., 2015; Sarvaramini et al., 2017; Xia et al., 2019; Mabudi et al., 2019; Xia et al., 2019). Specifically, the DFT method has recently enjoyed extensive application in this field, in an effort to understand the electronic structure and atomic structure of adsorbed surfactants (Wang et al., 2013; Geatches et al., 2013; Wang et al., 2015; Han et al., 2016; Liu et al., 2019).

Kaolinite is the main fine clay particle in coal slurry water, which has significant influence on the high efficiency solid-liquid separation of coal slurry water. In this study, four different methylamine cations (methyl primary amine cation (MPA^+ (CH_6N^+)), methyl secondary amine cation (MSA^+ ($C_2H_8N^+$)), methyl tertiary amine cation (MTA^+ ($C_3H_{10}N^+$)) and methyl quaternary amine cation (MQA^+ ($C_4H_{12}N^+$))) were constructed, and the single adsorption of different methylamine cation and competitive adsorption of methyl amine cation with water molecule on kaolinite basal surfaces were investigated using DFT calculations. The frontier orbital analysis, adsorption position analysis and adsorption energy calculation, adsorption configurations and bond populations, and charge analysis were presented and discussed. The adsorption mechanism is discussed in detail, which can provide a theoretical basis for developing new technology development and pharmaceutical design of sedimentation and clarification for coal slurry water.

2. Model and methods

Owing to fine kaolinite particles almost perfectly cleavaged along (001) basal surfaces (Vaz et al., 2002; Šolc et al., 2011) to form two different surfaces (Al-OH surface and Si-O surface), and these two different kaolinite basal surfaces were used as the main research objects in this study. DFT calculations of single adsorption and competitive adsorption on kaolinite basal surfaces were used with the CASTEP program in the software Material Studio 8.0, BIOVIA Corporation (Clark et al., 2005; Segall et al., 2002). The exchange-correlation function was used the Perdew, Burke, and Ernzerhof (PBE) functional with generalized gradient approximation (GGA) (Perdew et al., 1996), and the plane-wave cutoff was 400 eV. Grimme method (Zhang et al., 2012) was used for DFT-D dispersion corrections. The unbalanced charges in the adsorption systems of different methylamine cation adsorption on kaolinite basal surfaces are balanced by Cl- ions. The other specific parameter settings and computational method were implemented according to the process detailed by (Chen et al., 2019 a; Chen et al., 2019 b). The optimizations of different methylamine cations (MPA^+, MSA^+, MTA^+ and MQA^+) and water molecule were calculated in a 15 Å ×15 Å ×15 Å cubic box, and the optimization parameters were the same for primitive unit cell optimization. Fig. 1 and Fig. 2 illustrate the surface structure of kaolinite and the equilibrium configurations of different methylamine cation and water molecule, respectively.

The adsorption energies of different methylamine cation or water molecule on the kaolinite basal surfaces were calculated as:

$$E_{ads} = E_{total} - (E_{cation} + E_{surface}) \quad (1)$$

where E_{ads} is the adsorption energy, kJ/mol; E_{total} is the energy of the kaolinite basal surface with cation or (and) water molecule adsorbed, kJ/mol; $E_{cation/water}$ is the energy of different methylamine cation or water molecule in 15 Å×15 Å×15 Å cubic box, kJ/mol; and $E_{surface}$ is the energy of different kaolinite basal surface, kJ/mol.

The $Dmol^3$ module was used to calculate the frontier orbital properties of kaolinite basal surface and different methylamine cations with energy optimization, and the k points of Brillouin zone were sampled using Gamma point (Chen et al., 2020). Frontline orbit calculation parameters were as follows: exchange correlation function uses GGA-PBE, Effective Core Potentials and DNP basis sets,

the precision is set to fine, and the self-consistent field convergence criterion is set to 1.0×10^{-6} eV/atom.

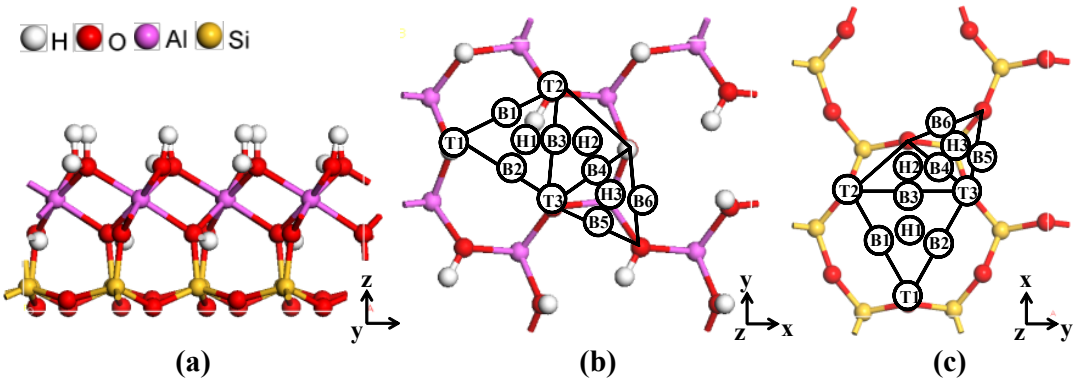

Fig. 1. Surface structure of kaolinite. (a) Layer structure; (b) Top view of (001) Al-OH surface with adsorption sites indicated; (c) Top view of Si-O surface with adsorption sites indicated. The adsorption sites are denoted as T (top positions), B (bridge positions), and H (hollow positions) in the picture

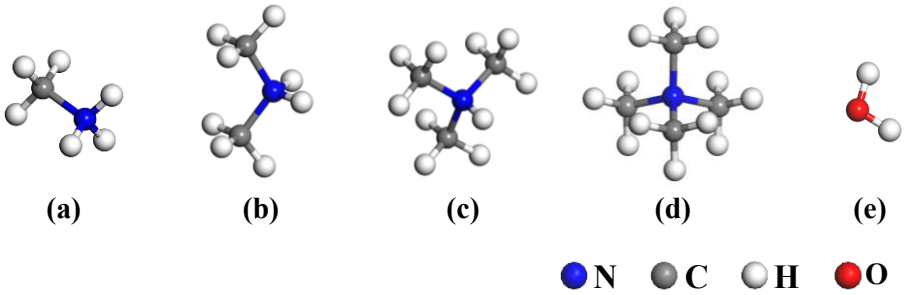

Fig. 2. Equilibrium configurations of different methylamine cation and water molecule. (a: MPA^+; b: MSA^+; c: MTA^+; d: MQA^+; e: H_2O)

3. Results and discussion

3.1. Frontier orbital analysis

According to frontier orbital theory, the smaller the absolute value of the energy difference (ΔE) between the highest occupied molecular orbital (HOMO) of one reactant and the lowest unoccupied molecular orbital (LUMO) of another reactant, the more easily the two reactants react (Chen et al., 2015). In order to understand the reactivity of each model and the optimal adsorption sites of cations on kaolinite basal surface, the frontier orbital energy differences of different methylamine cations and kaolinite were calculated. The results are summarizing in Table 1.

Table 1. Calculation of frontier orbital energy difference for different methylamine cation and kaolinite

Models	Frontier orbital energy /eV		Orbital energy difference /eV	
	HOMO	LUMO	ΔE_1	ΔE_2
MPA^+	-0.354	0.472	7.575	1.748
MSA^+	-0.153	0.616	7.719	1.949
MTA^+	0.021	0.698	7.801	2.213
MQA^+	0.278	0.743	7.846	2.380
Kaolinite	-7.103	-2.102	–	–

$\Delta E_1 = \left|E_{HOMO}^{surface} - E_{LUMO}^{adsorbate}\right|$, $\Delta E_2 = \left|E_{HOMO}^{adsorbate} - E_{LUMO}^{surface}\right|$; where $E_{HOMO}^{surface}$ and $E_{LUMO}^{surface}$ are the HOMO and LUMO energies of surface, respectively; $E_{HOMO}^{adsorbate}$ and $E_{LUMO}^{adsorbate}$ are the HOMO and LUMO energies of different methylamine cation, respectively.

It can be seen from Table 1 that the values of ΔE_2 are less than that of ΔE_1. Namely that, the HOMO of different methylamine cations and the LUMO of kaolinite can react easily. In this regard, the frontier orbital distribution of kaolinite and different methylamine cations were analyzed. Fig. 3 shows the LUMO of kaolinite, the yellow and blue portions in orbital graph represent α and β electrons in the spin, respectively, which are equivalent. The LUMO of kaolinite appears on the first layer of hydrogen atoms in the Al-OH surface, the hydrogen atoms in the lattice, and the oxygen atoms in each layer, and the intensity of the hydrogen atoms is the largest, while the intensity on the oxygen atoms of each layer is uniform but very small.

Fig. 4 shows the HOMO of different methylamine cations. It is observed that the HOMO of different methylamine cations appears on the head hydrogen atom (H_N) and have the highest intensity at this position (Fig. 4 (a)~(c)). Then the HOMO of the methyl quaternary amine cation appears in the triangular region composed of three adjacent methyl hydrogen atoms (Fig. 4 (d)). Since the LUMO of kaolinite has the highest intensity on the first layer of hydrogen atoms on the Al-OH surface, different methylamine cations should be more easily adsorbed on the kaolinite (001). This is what frontier orbital theory asserts, but the actual adsorption should also consider hydrogen bondings and other interactions, for example electrostatic interaction.

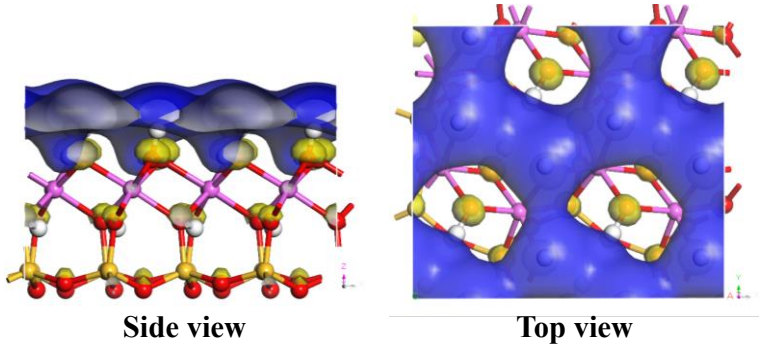

Fig. 3. The LUMO of kaolinite, the isovalue is 0.02 electrons/Å^3

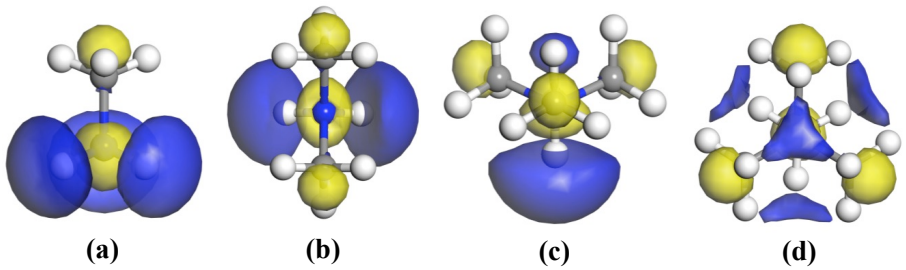

Fig. 4. The HOMO of different methylamine cation, the isovalue is 0.05 electrons/Å^3. (a: MPA$^+$; b: MSA$^+$; c: MTA$^+$; d: MQA$^+$)

3.2. Single adsorption

The adsorption energies of different methylamine cation on different initial position of kaolinite basal surfaces were calculated as shown in Table 2. The adsorption energies of different methylamine cation on kaolinite Al-OH surface and Si-O surface were -128.654~-66.058 and -140.961~-78.537 kJ/moL, respectively. Which are significantly lower than that of water molecule on kaolinite Al-OH surface (-72.12~-19.23 kJ/moL) and Si-O surface (-19.23~-5.77 kJ/moL) (Chen et al., 2019b), indicating that these four different methylamine cations can also be stably adsorbed on kaolinite basal surfaces when water molecule compete for adsorption. The optimal adsorption position of MPA$^+$, MSA$^+$, MTA$^+$ and MQA$^+$ on kaolinite Al-OH surface appeared at the H3 position, and the adsorption energies were -125.385, -126.154, -128.654 and -109.711 kJ/mol, respectively. Furthermore, the optimal adsorption position of MPA$^+$, MSA$^+$, MTA$^+$ and MQA$^+$ on the kaolinite Si-O surface appeared at the H1 position, while the adsorption energies were -140.961, -136.154, -138.558 and -115.961 kJ/mol, respectively. Namely that the adsorption energies of three methyl amine cation (MPA$^+$, MSA$^+$ and MTA$^+$) on kaolinite basal

surfaces did not differ significantly, but they are lower than that of methyl quaternary amine cation (MQA^+) on kaolinite basal surfaces. It is indicating that the methylamine cations are more stable than the methyl quaternary amine cation adsorption on kaolinite basal surfaces. The adsorption energies of different methylamine cation on kaolinite Al-OH surface are significantly higher than that on the kaolinite Si-O surface, which means that the adsorptions of different methylamine cation on kaolinite Si-O surface are more stable, (Geatches et al., 2012) reported the similar results.

Table 2. Adsorption energies of different methylamine cation on initial position of kaolinite basal surfaces

Adsorption configuration	Al-OH surface			Si-O surface		
	Initial position	Final position	Eads / kJ·moL^{-1}	Initial position	Final position	Eads / kJ·moL^{-1}
CH_6N^+	H1	H1	-90.152	H1	H1	-140.961
	H2	H2	-109.769	H2	H2	-121.435
	H3	H3	-125.385	H3	H3	-112.473
$C_2H_8N^+$	B1	B1	-103.235	B1	B1	-125.356
	B2	B2	-105.354	B2	B2	-123.443
	B3	B3	-103.077	B3	H1	-136.154
	B4	B4	-118.734	B4	B4	-116.431
	B5	B5	-113.173	B5	B5	-113.575
	B6	H3	-126.154	B6	B6	-115.324
$C_3H_{10}N^+$	T1	T1	-98.942	T1	T1	-127.543
	T2	T2	-121.442	T2	H1	-138.558
	T3	H3	-128.654	T3	T3	-132.454
$C_4H_{13}N^+$	H1	H1	-66.058	H1	H1	-115.961
	H2	H2	-88.654	H2	H2	-93.435
	H3	H3	-109.711	H3	H3	-78.537

According to the results in Table 2, the optimal configurations of different methylamine cation on kaolinite Al-OH surface (H3) and Si-O surface (H1) were taken as examples. The optimum configurations of different methylamine cation adsorbed on kaolinite basal surface are shown in Fig. 5 and Fig. 6, respectively. The dotted lines in blue and black represent N-H…O strong hydrogen bonds and C-H…O weak hydrogen bonds, respectively. As shown in these two figures, the three methylamine cations of MPA^+, MSA^+ and MTA^+ form 1, 2 and 3 N-H...O strong hydrogen bonds with kaolinite basal surface, respectively. Meanwhile the methyl quaternary amine cation of MQA^+ forms 3 C-H...O weak hydrogen bonds with kaolinite basal surface.

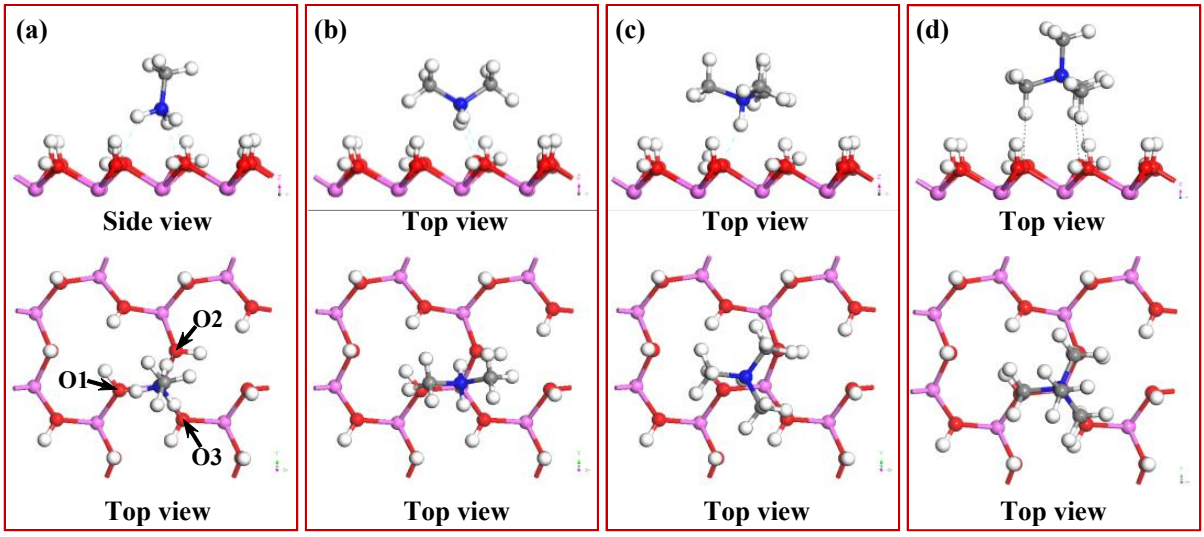

Fig. 5. Optimum configurations of different methylamine cation adsorbed on kaolinite Al-OH surface. (a: MPA^+; b: MSA^+; c: MTA^+; d: MQA^+)

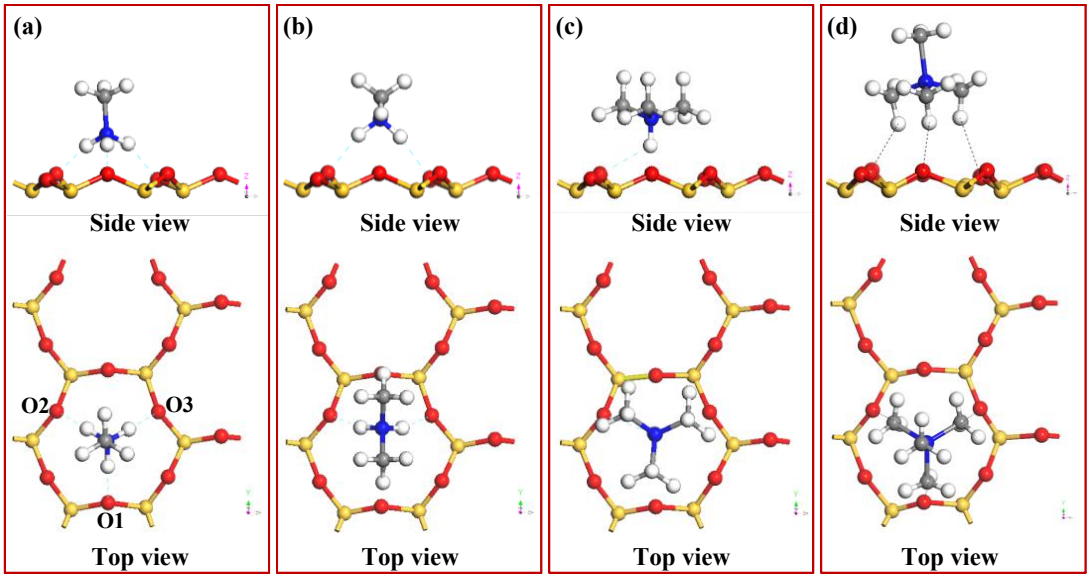

Fig. 6. Optimum configurations of different methylamine cation adsorbed on kaolinite ($00\bar{1}$) surface. (a: MPA^+; b: MSA^+; c: MTA^+; d: MQA^+)

Table 3 shows the Mulliken bond populations of different methylamine cation adsorbed on kaolinite basal surfaces. In the optimum configurations of different methylamine cation on kaolinite Al-OH surface, the hydrogen bond lengths are 1.770~2.212 Å, while the Mulliken bond population values are in the 0.03~0.09 range. Meanwhile the hydrogen bond lengths are 1.775~2.481 Å and the Mulliken bond population values are 0.02~0.09 for the different methylamine cation on the kaolinite Si-O surface. The shorter the bond length, the larger the Mulliken bond population value, and subsequently the stronger the interaction between atoms. The bond lengths of the C-H...O weak hydrogen bonds formed between methyl quaternary amine cation and kaolinite basal surfaces are significantly larger than that of the N-H…O strong hydrogen bonds formed between methyl amine cation and kaolinite basal surfaces. The result indicating the interactions between these methyl amine cations and kaolinite basal surfaces are stronger than that between the methyl quaternary amine cations and kaolinite basal surfaces.

Table 3. Mulliken bond populations of different methylamine cation adsorbed on kaolinite basal surfaces

Adsorption configuration	Al-OH surface			Si-O surface		
	Bond	Length /Å	Bond population	Bond	Length /Å	Bond population
MPA^+	N-H1…O1	2.082	0.03	N-H1…O1	1.828	0.09
	N-H1…O2	1.770	0.09	N-H1…O2	1.775	0.09
	N-H3…O3	1.962	0.05	N-H3…O3	1.951	0.06
MSA^+	N-H1…O1	1.840	0.09	N-H2…O2	1.959	0.06
	N-H2…O2	2.200	0.03	N-H3…O3	2.038	0.03
MTA^+	N-H1…O1	1.898	0.09	N-H1…O1	2.410	0.02
MQA^+	C-H1…O1	2.212	0.03	C-H1…O1	2.118	0.03
	C-H2…O2	2.188	0.03	C-H2…O2	2.214	0.03
	C-H3…O3	2.153	0.03	C-H3…O3	2.481	0.02

The oxygen atomic numbers in Table 3 are corresponding to that in Fig. 5 and Fig. 6, and the hydrogen atoms forming hydrogen bonds with corresponding oxygen atoms are denoted as H1, H2 and H3, respectively; the same below.

Fig. 7 reveal the electron density difference of MPA^+ adsorbed on the kaolinite basal surfaces. The blue and yellow area in this figure represents the electron accumulation and electron depletion,

respectively. It is important to note here that the magnitude of the interaction between different methylamine cation and kaolinite basal surface is approximately proportional to the range of electron accumulation and depletion in adsorption system. After the adsorption of MPA^+ on the kaolinite basal surfaces, there is a large amount of charge transfer. And the electrons transferred from MPA^+ to the kaolinite basal surface. The electron accumulation mainly distributed around the hydrogen atoms in cation (H_A), and electron depletion mainly distributed around the oxygen atoms of kaolinite basal surface (O_S). At the same time, it can be seen that the electron rearrangement range between adjacent atoms in adsorption configurations of kaolinite Al-OH surface is significantly smaller than that in adsorption configurations of kaolinite Si-O surface. This suggests the interactions of different methylamine cations on the kaolinite Al-OH surface are weaker than that on the kaolinite Si-O surface. This finding is very consistent with the calculation of adsorption energy.

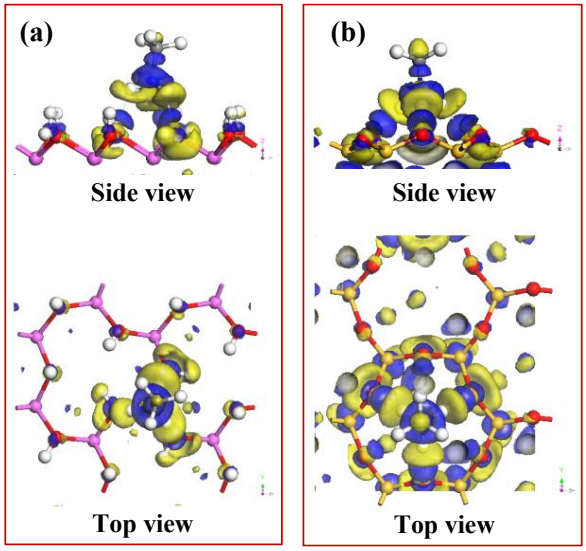

Fig. 7. Electron density difference of the optimum adsorption configurations of MPA^+ adsorbed on kaolinite basal surfaces, the isosurface value is 0.01 electrons/ $Å^3$. (a: Al-OH surface; b: Si-O surface)

The Mulliken charge populations of the atoms before and after different methylamine cations adsorption on kaolinite basal surfaces are shown in Table 4. In the adsorption configurations of cations on the kaolinite Al-OH surface, the H_A atoms lose 0.01-0.15 e electrons, and the charge of the O_S atoms forming hydrogen bonds with them does not change or loses a small number of electrons. Indicating that, after different methylamine cations adsorbed on the kaolinite Al-OH surface, the electrons are not only transferred to the O_s atoms, but also transferred to the other atoms of kaolinite Al-OH surface which are adjacent to the cation (see Fig. 7). In the adsorption configurations of different methylamine cations on kaolinite Si-O surface, the H_A lose 0.05-0.17 e electrons, and the O_s atoms forming hydrogen bonds with them get 0.10-0.20 e electrons. Indicated here is the fact that the electron transfer of different methylamine cations after adsorption on kaolinite Si-O surface mainly occurs between the H_A and the O_s atoms forming hydrogen bonds with the cations. The number of charges lost by the cations of different methylamine cations before and after adsorption on the kaolinite Al-OH surface and Si-O surface confirms that the number of charges lost by different amine cations is not much different. They are, however, larger than that lost by quaternary ammonium cations. The number of charges lost in different methylamine cations after adsorption on the kaolinite Al-OH surface is smaller than that in different methylamine cations after adsorption on the Si-O surface. This outcome is consistent with the results concerning the electron density difference.

The adsorption configurations and charge analysis of MPA^+ adsorbed on the kaolinite basal surface indicate that the adsorption mechanism of methylamine cations on this surface mainly takes the form of hydrogen bonding and electrostatic attraction. Of these electrostatic attraction takes the dominant position and this is the main reason why the calculation results of adsorption energy are inconsistent with the frontier orbital analysis. First, the methylamine cations mainly form hydrogen bonds between the O_s atoms and the H_A (H atom in cations) atoms, while the first layer of H_s atoms of

the kaolinite Al-OH surface produces a certain degree of steric hindrance to the formation of the hydrogen bond of $H_A...O_s$. Secondly, the O_s atoms of kaolinite Si-O surface are also distributed with a certain intensity of LUMO orbitals, which also react with methylamine cations. Meanwhile, according to Mulliken charge analysis, the O_s atoms of the kaolinite Al-OH surface and Si-O surface have a large amount of negative charge, which has a strong electrostatic attraction to the methylamine cations. Meanwhile each O_s atom on the kaolinite Al-OH surface has an H_s atom, which causes the electrostatic attraction between kaolinite Al-OH surface and cations to be weaker than that between kaolinite Si-O surface and cations.

Table 4. Mulliken charge populations of atoms before and after different methylamine cations adsorption on kaolinite basal surfaces

Atomic number	Adsorption states	Mulliken charges /e	
		Al-OH surface	Si-O surface
H1	before	0.28	0.28
	after	0.41	0.43
H2	before	0.28	0.28
	after	0.40	0.43
H3	before	0.28	0.28
	after	0.40	0.44
O1	before	-1.06	-1.06
	after	-1.02	-1.15
O2	before	-1.06	-1.06
	after	-0.99	-1.15
O3	before	-1.05	-1.05
	after	-1.02	-1.16
MPA^+	before	0	0
	after	0.51	0.75
Kaolinite basal surface	before	0	0
	after	-0.51	-0.75

3.3. Competitive adsorption

Taking the methyl primary amine cation with the best adsorption effect as an example, the competitive adsorptions of methylamine cation and water molecule on kaolinite basal surfaces were simulated, the results are shown in Fig. 8 and Fig. 9.

Fig. 8 shows the competitive adsorption of MPA^+ and water on kaolinite Al-OH surface. From the comparative analysis of Fig. 8 (a) and (b), MPA^+ and water molecule adsorbed on kaolinite Al-OH surface mainly by forming hydrogen bonds. In addition, the MPA^+ and water molecule are slightly offset from each other to the two sides, which means that the methylamine cations can flush out the surrounding water molecules to get rid of their steric effect and stably adsorb on the kaolinite Al-OH surface. This is very evident when MPA^+ competes for adsorption with water molecules. As shown in Fig. 8 (c), a large amount of electron transfer occurs in the system after adsorption equilibrium. The electron transfer of MPA^+ mainly occurs around $-NH_3$ while the electron transfer occurs around all the water molecules. Fig. 9 shows the competitive adsorption of MPA^+ and water adsorbed on the kaolinite Si-O surface. Here the competitive adsorption law is similar to the adsorption law regarding the kaolinite Al-OH surface, the difference being that the electron transfer range in the competitive adsorption of kaolinite Si-O surface is slightly larger than that of kaolinite Al-OH surface. Specifically, the stability of MPA^+ and water molecules' competitive adsorption on the kaolinite Si-O surface is stronger.

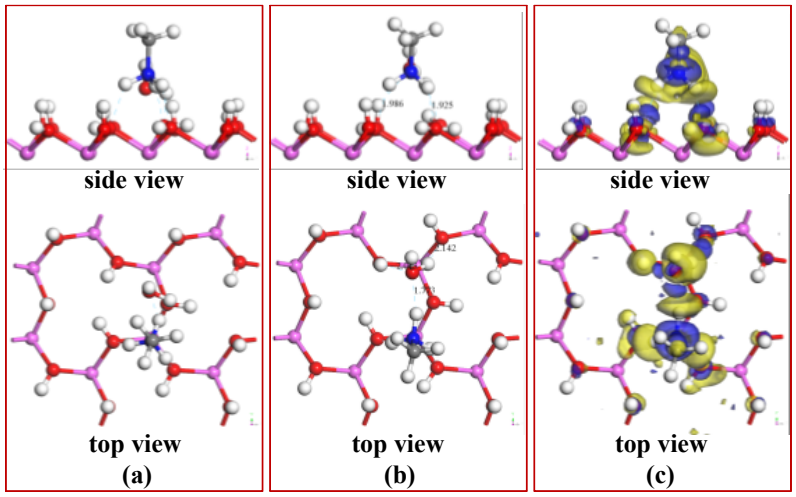

Fig. 8. Competitive adsorption of MPA^+ and water adsorbed on kaolinite Al-OH surface. (a: Original configuration; b: Equilibrium configuration; c: The electron density difference, the isosurface value is 0.006 electrons/ $Å^3$)

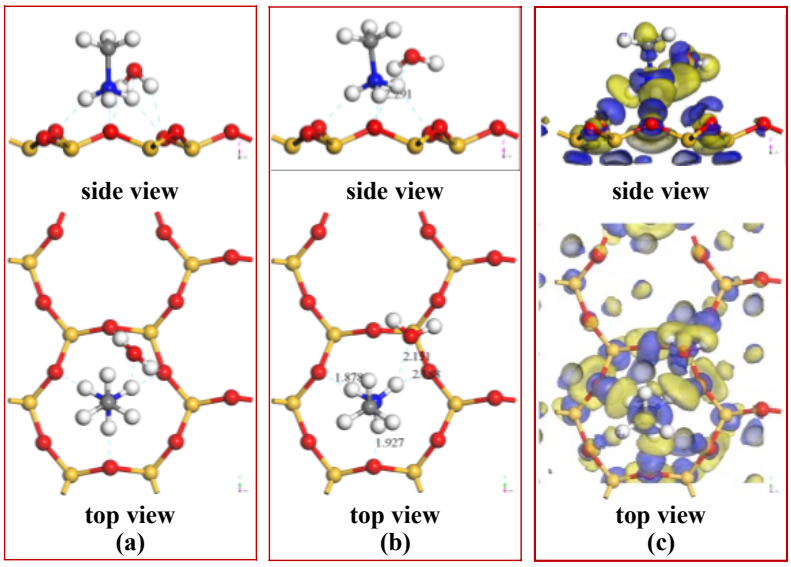

Fig. 9. Competitive adsorption of MPA^+ and water adsorbed on kaolinite Si-O surface. (a: Original configuration; b: Equilibrium configuration; c: The electron density difference, the isosurface value is 0.01 electrons/ $Å^3$)

Table 5 shows the adsorption energies and Mulliken charge populations on the competitive adsorption of MPA^+ and water adsorbed on kaolinite basal surfaces. According to the results for adsorption energy calculation summarized in Table 5, the total adsorption energy of MPA^+ and water molecule on kaolinite Al-OH surface is -210.32 kJ/moL, which is significantly lower than that on kaolinite Si-O surface (-216.22 kJ/moL). Indicating that the competitive adsorption system of kaolinite Si-O surface is more stable. Compared to the adsorption energies of single MPA^+ on kaolinite basal surfaces in Table 2 (-125.385 and -140.961 kJ/moL, respectively), suggesting that the adsorption state of the competitive adsorption system is more stable.

From the results of the Mulliken charge populations in Table 5, it can be seen that in the competition for adsorption on the kaolinite Al-OH surface, the water molecule and kaolinite Al-OH surface received 0.11 and 0.44 e electrons, respectively, and MPA^+ lost 0.55 e electrons. In the competition for adsorption on the kaolinite Si-O surface, the water molecule charge is unchanged, the Si-O surface received 0.80 e electrons, and MPA^+ lost 0.80 e, respectively. Furthermore,. the total charge transfer amounts resulting from the competition for adsorption on the kaolinite Al-OH surface and Si-O surface were 0.55 and 0.80 e, respectively. This outcome is very consistent with the

adsorption energy calculation. At the same time, according to the analysis done on the Mulliken charge populations of water molecules in different competitive adsorption systems, these water molecules received electrons by interacting with MPA^+ while losing electrons by hydrogen bonding with kaolinite basal surface (Chen, 2017). Subsequently, the interaction of single MPA^+ on the surface is smaller, indicating that water molecules to a certain extent inhibit the adsorption of MPA^+ on kaolinite basal surfaces.

Comprehensive analysis shows that the methylamine cations can adsorb on kaolinite basal surfaces by electrostatic interaction and hydrogen bonds, and realize the effective surface hydrophobic modification of kaolinite particles by its hydrophobic polar groups, which can provide a theoretical basis to synthetic new surfactants and develop new technologies of sedimentation and clarification for high muddied coal slurry water.

Table 5. Adsorption energies and Mulliken charge populations on the competitive adsorption of MPA^+ and water adsorbed on kaolinite basal surfaces

Adsorption configuration	Eads / kJ·moL^{-1}	Adsorption states		Mulliken charges /e
MPA^+ / Al-OH surface	-210.32	H_2O	before	0
			after	-0.11
		MPA^+	before	0
			after	0.55
		Surface	before	0
			after	-0.44
MPA^+ / $(00\bar{1})$ surface	-216.22	H_2O	before	0
			after	0
		MPA^+	before	0
			after	0.80
		Surface	before	0
			after	-0.80

4. Conclusions

(1) The results of frontier orbital analysis indicate that the HOMO orbitals of methylamine cations should react more easily with the LUMO orbitals of kaolinite.

(2) Different methylamine cations MPA^+, MSA^+, MTA^+ and MQA^+ can form hydrogen bonds of N-H...O or C-H...O with the kaolinite basal surface. The best adsorption sites for methylamine cations on the kaolinite Al-OH surface are in H3 position, and the adsorption energies were -125.385, -126.154, -128.654 and -109.711 kJ/mol, respectively. The best adsorption sites for methylamine cations on the kaolinite Si-O surface are H1, and the adsorption energies were -140.961, -136.154, -138.558 and -115.961 kJ/mol, respectively. It was evident that the methylamine cations were more easily adsorbed on the kaolinite Si-O surface.

(3) Different methylamine cations are more easily adsorbed on the kaolinite Si-O surface, which is contrary to what frontier orbital analysis asserts. The main explanation is that the adsorption mechanism of different methylamine cation adsorbed on kaolinite basal surfaces is mainly hydrogen bonds and electrostatic attraction, in which the electrostatic attraction plays the main role.

(4) In the presence of competitive adsorption with water molecule, the methylamine cation is capable of flushing out the surrounding water molecule to get rid of its steric effect and stably adsorbing on kaolinite basal surfaces, and the adsorption state of the competitive adsorption system is more stable.

Acknowledgments

The financial supports for this work from the National Natural Science Foundation of China under the grant No. 51804009 and the grant No. 51874011 are gratefully acknowledged.

References

BERGAYA, F., LAGALY, G., 2013. *Chapter 1-general introduction: clays, clay minerals, and clay science.* in: Faïza, B., Gerhard, L. (Eds.), Developments in Clay Science, vol. 5, Elsevier.

CHEN, J.H., 2015. *The solide physics of sulphide minerals flotation*. Central South University Press: Hunan, 61-62.

CHEN, J., 2017. *Characteristics and mechanism research on hydrophobic aggregation of fine particles in high muddied coal slurry water.* Anhui University of Science and Technology,96-102.

CHEN, J., MIN, F., LIU, L., CAI, C., 2020. *Systematic exploration of the interactions between Fe-doped kaolinite and coal based on DFT calculations.* Fuel. 266,117082.

CHEN, J., MIN, F., LIU, L., 2019a. *The interactions between fine particles of coal and kaolinite in aqueous, insights from experiments and molecular simulations.* Appl. Surf. Sci. 467-468,12-21.

CHEN, J., MIN, F., LIU, L., LIU, C., 2019b. *Mechanism research on surface hydration of kaolinite, insights from DFT and MD simulations.* Appl. Surf. Sci. 476,6-15.

CHEN, J., MIN, F., LIU, L., LIU, C., LU, F., 2017. *Experimental investigation and DFT calculation of different amine/ammonium salts adsorption on kaolinite.* Appl. Surf. Sci. 419,241-251.

CHEN, J., MIN, F., LIU, L., PENG, C., LU, F., 2016. *Hydrophobic aggregation of fine particles in high muddied coal slurry water.* Water Sci. Technol. 73, 501-510.

CLARK, S.J., SEGALL, M.D., PICKARD, C.J., HASNIP, P.J., PROBERT, M.I.J., REFSON, K., PAYNE, M.C., 2005. *First principles methods using CASTEP. Z.* Kristallogr. 220,567-570.

GEATCHES, D.L., CLARK, S.J., GREENWELL, H.C., 2013. *DFT+U investigation of the catalytic properties of ferruginous clay.* Am. Mineral. 98,132-140.

GEATCHES, D.L., JACQUET, A., CLARK, S.J., GREENWELL, H.C., 2012. *Monomer Adsorption on Kaolinite: Modeling the Essential Ingredients.* J. Phys. Chem. C, 116,22365-22374.

GIBSONA, B., WONYENA, D.G., CHEHREH, C.S., 2017. *A review of pretreatment of diasporic bauxite ores by flotation separation.* Miner. Eng.114,64-73.

HAN, Y., LIU, W., CHEN, J., 2016. *DFT simulation of the adsorption of sodium silicate species on kaolinite basal surfaces.* Appl. Surf. Sci. 370,403-409.

HUANG, Q., LI, X., REN, S., LUO, W., 2019. *Removal of ethyl, isobutyl, and isoamyl xanthates using cationic gemini surfactant-modified montmorillonites.* Colloids Surf. A. 580,123723.

HU, Y., LIU, L., MIN, F., ZHANG, M., SONG, S., 2013. *Hydrophobic aggregation of colloidal kaolinite in aqueous suspensions with dodecylamine.* Colloid. Surface, A. 434,281-286.

JELDRES R.I., URIBE, L., CISTERNAS, L.A., GUTIERREZ, L., LEIVA, W.H., VALENZUELA, J., 2019. *The effect of clay minerals on the process of flotation of copper ores: A critical review.* Appl. Clay. Sci. 170,57-69.

JIANG, H., SUN, Z., LONG, H., HU, Y., HUANG, K., ZHU, S., 2014. *A comparison study of the flotation and adsorption behaviors of diaspore and kaolinite with quaternary ammonium collectors.* Miner. Eng. 65, 124-129.

LEE, K.E., MORAD, N., POH, B.T., TENG, T.T., 2011. *Comparative study on the effectiveness of hydrophobically modified cationic polyacrylamide groups in the flocculation of kaolin*. Desalination. 270, 206-213.

LIU, L., MIN, F., CHEN, J., LU, F., SHEN, L., 2019. *The adsorption of dodecylamine and oleic acid on kaolinite basal surfaces: Insights from DFT calculation and experimental investigation*. Appl. Surf. Sci. 470, 27-35.

LIU, S., CHEN, X., LAUTEN, R.A., PENGA, Y., LIU, Q., 2018. *Mitigating the negative effects of clay minerals on gold flotation by a lignosulfonate-based biopolymer.* Miner. Eng. 126,9-15.

LIU, D., EDRAKI M., BERRY L., 2018. *Investigating the settling behavior of saline tailing suspensions using kaolinite, bentonite, and illite clay minerals.* Powder Technol.326,228-236.

MABUDI, A., NOAPARAST, M., GHARABAGHI, M., VASQUEZ, V.R., 2019. *Polystyrene nanoparticles as a flotation collector: A molecular dynamics study.* J. Mol. Liq. 275,554-566.

MIN, F., PENG, C., SONG, S., 2014. *Hydration layers on clay mineral surfaces in aqueous solutions: A review.* Arch. Min. Sci. 59,373-384.

MIN F., REN B., CHEN J., LIU, C., PENG, C., 2020. Mechanism and experimental study on promoting coal slime dewatering based on weakening of hydration layer. J.China Coal Soc. 45(1),368 - 376

PENDHARKER, S., SHENDE, S., JACOB, Z., NAZEMIFARD, N., 2017. *Three-dimensional optical tomography of bitumen and clay association in oil sands tailings.* Fuel. 207,262-267.

PENG, C., ZHONG, Y., MIN, F., 2018. *Adsorption of alkylamine cations on montmorillonite Al-OH surface: A density functional theory study.* Appl. Clay. Sci. 152,249-258.

PERDEW, J.P., BURKE, K., ERNZERHOF, M., 1996. *Generalized gradient approximation made simple.* Phys. Rev. Lett. 77,3865-3868.

RATH, S.S., SAHOO, H., DAS, B., MISHRA, B.K., 2014. *Density functional calculations of amines on the (101) face of quartz.* Miner. Eng. 69,57-64.

RODRIGUES, O.M.S., PERES, A.E.C., MARTINS, A.H., PEREIRA, C.A., 2013. *Kaolinite and hematite flotation separation using etheramine and ammonium quaternary salts.* Miner. Eng. 40,12-15.

SEGALL, M.D., LINDAN, P.J.D., PROBERT, M.J., PICKARD, C.J., HASNIP, P.J., CLARK, S.J., PAYNE, M.C., 2002. *First-principles simulation: ideas, illustrations and the CASTEP code.* J. Phys.: Condens. Matter. 14, 2717-2744.

SARVARAMINI, A., LARACHI, F., 2017. *Understanding the interactions of thiophosphorus collectors with chalcopyrite through DFT simulation.* Comput. Mater. Sci. 132,137-145.

SHEN, L., ZHU, J., LIU, L., WANG, H., 2017. *Flotation of fine kaolinite using dodecylamine chloride/fatty acids mixture as collector.* Powder Technol. 312,159-165.

ŠOLC, R., GERZABEK, M.H., LISCHKA, H., TUNEGA D., 2011. *Wettability of kaolinite basal surfaces - Molecular dynamic study.* Geoderma. 169,47-54.

WANG, X., HUANG, Y., PAN, Z., WANG, Y., LIU, C., 2015. *Theoretical investigation of lead vapor adsorption on kaolinite basal surfaces with DFT calculations.* J. Hazard. Mater. 295,43-54.

WANG, X., QIAN, P., SONG, K., ZHANG, C., DONG, J., 2013. *The DFT study of adsorption of 2,4-dinitrotoluene on kaolinite basal surfaces.* Comput. Theor. Chem. 1025,16-23.

WANG, L., HU, Y., SUN, W., SUN, Y., 2015. *Molecular dynamics simulation study of the interaction of mixed cationic/anionic surfactants with muscovite.* Appl. Surf. Sci. 327,364-370.

XIA Y., YANG Z., ZHANG R., XING Y., GUI X., 2019a. *Enhancement of the surface hydrophobicity of low-rank coal by adsorbing DTAB: An experimental and molecular dynamics simulation study.* Fuel.239,145-152.

XIA, Y., ZHANG, R., XING, Y., GUI, X., 2019b. *Molecular dynamics simulation of uranyl(VI) adsorption equilibria onto an external montmorillonite surface.* Fuel. 235,687-695.

XING Y., XU X., GUI X., CAO Y., XU M., 2017. *Effect of kaolinite and montmorillonite on fine coal flotation.* Fuel. 195,284-289.

XIONG, F., JIANG, Z., LI, P., WANG, X., BI, H., LI, Y., WANG, Z., AMOOIE, M.A., SOLTANIAN, M.R., MOORTGAT, J., 2017. *Pore structure of transitional shales in the Ordos Basin, NW China: effects of composition on gas storage capacity.* Fuel. 206,504-515.

YU Y., MA L., CAO M., LIU Q., 2017. *Slime coatings in froth flotation: A review.* Miner. Eng. 114,26-36.

ZHANG, G., AI-SAIDI, W.A., MYSHAKIN, E.M., JORDAN, K.D., 2012. *Dispersion-Corrected DFT and classical force field calculations of water loading on a clay surface.* J. Phys. Chem. C. 116,17134-17141.

ZHANG, N., EJTEMAEI, M., NGUYEN, A.V., ZHOU, C., 2019. *XPS analysis of the surface chemistry of sulfuric acid-treated kaolinite and diaspore minerals with flotation reagents.* Miner. Eng. 136,1-7.

ZHAO, H., LI, Y., SONG, Q., LIU, S., MA, Q., MA, L., SHU, X., 2019a. *Catalytic reforming of volatiles fromco-pyrolysis of lignite blended with corn straw over three different structures of iron ores.* J. Anal. Appl. Pyrol. 144:104714.

ZHAO, H., LI, Y., SONG, Q., LIU, S., YAN, J., MA, Q., MA, L., SHU, X., 2019b. *Investigation on the thermal behavior characteristics and products composition of four pulverized coals: Its potential applications in coal cleaning.* Int. J. Hydrogen Energy. 44,23620–23638.

ZHAO, H., SONG, Q., LIU, S., LI, Y., WANG, X., SHU, X., 2018. *Study on catalytic co-pyrolysis of physical mixture/staged pyrolysis characteristics of lignite and straw over an catalytic beds of char and its mechanism.* Energy Convers. Manage. 161,13–26.

VAZ, C.M.P., HERRMANN, P.S.P., CRESTANA, S., 2002. *Thickness and size distribution of clay-sized soil particles measured through atomic force microscopy.* Powder Technol. 126,51-58.